Available online at www.sciencedirect.com
ScienceDirect
Journal of Power Sources 159 (2006) 179–185
JOURNAL OF POWER SOURCES
www.elsevier.com/locate/jpowsour

# Effect of annealing temperature on electrochemical performance of thin-film $LiMn_2O_4$ cathode

Fu-Yun Shih, Kuan-Zong Fung *

*Department of Materials Science and Engineering, National Cheng Kung University, Tainan 70101,Taiwan*

Available online 5 June 2006

**Abstract**

Spinel $LiMn_2O_4$ thin-film cathodes were obtained by spin-coating the chitosan-containing precursor solution on a Pt-coated silicon substrate followed by a two-stage heat-treatment procedure. The $LiMn_2O_4$ film calcined at 700 °C for 1 h showed the highest Li-ion diffusion coefficient, $1.55 \times 10^{-12}$ cm$^2$ s$^{-1}$ (PSCA measurement) among all calcined films. It is attributed to the larger interstitial space and better crystal perfection of $LiMn_2O_4$ film calcined at 700 °C for 1 h. Consequently, the 700 °C-calcined $LiMn_2O_4$ film exhibited the best rate performance in comparison with the ones calcined at other temperatures.


*Keywords:* Thin film; $LiMn_2O_4$; Li-ion diffusion coefficient; Annealing temperature; Chitosan

## 1. Introduction

Crystalline $LiMn_2O_4$ is one of the most extensively investigated cathode materials for thin-film microbatteries because of its advantages of less toxicity, lower cost, easier preparation and high operating voltage. Nowadays, $LiMn_2O_4$ thin films have been fabricated by several methods, such as R.F. magnetron sputtering, pulse laser deposition and electrostatic spray deposition [1–6]. However, most of these methods need expensive apparatuses or are difficult to give the deposited films with accurate stoichiometry.

The solution-based route is an alternative procedure for the deposition of thin-film $LiMn_2O_4$ cathodes owing to its simple and easy process [7–9]. Chitosan is a polysaccharide derived from crustacean and fungal chitin. Due to its low-toxicity and tissue-compatibility, chitosan has been used in pharmaceutics, medicine and food industry for the last few decades. In our previous work [10], the addition of chitosan to the lithium/manganese acetates containing precursor solution was found to be helpful to deposition of $LiMn_2O_4$ films. Thus, in order to facilitate the deposition of $LiMn_2O_4$ films on a Pt-coated silicon substrate, the lithium/manganese acetates-containing precursor solution with chitosan addition was used as a coating solution.

However, a systematic investigation regarding the effect of annealing temperature on the electrochemical performance of $LiMn_2O_4$ films deposited from sol–gel method was limited. Insight into the kinetic property of $LiMn_2O_4$ during Li-ion intercalation and extraction is a key issue for the electrochemical performance of thin-film microbatteries, which is strongly dominated by the annealing condition. Thus, in the present study, the effect of annealing temperature on the Li ion diffusivity of the deposited $LiMn_2O_4$ films was carefully investigated.

## 2. Experimental

0.025 mol lithium acetate (Alfa Aesar, 99%) and 0.05 mol manganese acetate (Fluka, 99%) were dissolved in 25 ml ethanol (Fluka, 99.8%). Then, 0.125 g chitosan (Fluka, low viscous) was also dissolved in 25 ml de-ionized water containing 1.5 ml acetic acid (Fluka, 99.8%). Subsequently, the ethanol solution with acetate salts was mixed with the aqueous solution containing chitosan and stirred for 2 h. The Li–Mn–O–chitosan precursor films were deposited on a Pt-coated substrate by spin-coating the well-prepared precursor solution at a spinning speed of 3000 rpm. The deposited films were then calcined at 300 °C for 1 h at the first stage and subsequently at higher temperatures (400–800 °C) for another 1 h at the second stage. As is evidenced in our previous work [10], a dense $LiMn_2O_4$ thin-film cathode could be obtained via such a preparation process.

* Corresponding author. Tel.: +886 6 2756402; fax: +886 6 2380208.
*E-mail address:* kzfung@mail.ncku.edu.tw (K.-Z. Fung).

0378-7753/$ – see front matter © 2006 Elsevier B.V. All rights reserved.
doi:10.1016/j.jpowsour.2006.04.040

Film thickness was measured by a contact probe surface profilometer (Tencor Instruments Alpha-step 200). The phase identification of the prepared films was characterized by glancing-angle X-ray diffraction (GXRD) using Rigaku D/MAX 2500 diffractometer with Cu Kα radiation at a glancing incident angle of 1° and a scanning rate of 4° $min^{-1}$. Moreover, the calcined $LiMn_2O_4$ films were also scraped off from the silicon substrate and collected for the determination of the lattice parameter. The evaluation of the lattice parameter was carried out using Rigaku Rad II diffractometer with Cu Kα radiation at a scanning rate of 0.25° $min^{-1}$. Si powder was used as an internal standard. Lattice parameter was fitted via the least square procedure.

The evaluation of Li-ion diffusion coefficient for the deposited $LiMn_2O_4$ films calcined at different temperatures was carried out using both cyclic voltammetry (CV) and potential step chronoamperometry (PSCA) methods at room temperature. A three-electrode cell was employed for electrochemical measurements using lithium foil as counter and reference electrodes and the deposited $LiMn_2O_4$ films as working electrodes. The electrolyte was a mixed solution of ethylene carbonate (EC) and diethyl carbonate (DEC) (1:1 in volume) containing 1 M $LiPF_6$ (Mitsubishi Chemical). In this work, unless stated otherwise, the deposited $LiMn_2O_4$ thin-film cathodes were about $0.5 \pm 0.05$ μm in thickness and the electrode area inside the electrolyte solution was 1 $cm^2$. Both CV and PSCA measurements were carried out by employing an EG&G electrochemical analysis system (model 273A).

## 3. Results and discussion

### 3.1. X-ray diffraction analysis of the deposited films

Fig. 1 shows the GXRD traces of Li–Mn–O–chitosan precursor films calcined at temperatures ranging from 400 to 900 °C for 1 h. For the sample calcined at 400 °C for 1 h (Fig. 1a), the peaks located at $2\theta = 18.64$, 36.26, 44.10 and 58.41° correspond to the (1 1 1), (3 1 1), (4 0 0) and (5 1 1) diffraction reflections of spinel $LiMn_2O_4$ lattice (JCPDS 89-0118). The observed peaks became sharper with increasing the calcination temperature to 700 °C, indicating that a $LiMn_2O_4$ film with better crystallinity was obtained at the temperature of 700 °C. On the other hand, some additional peaks at $2\theta = 18.2$, 28.82 and 32.31° appeared when the temperature was raised to 800 °C. With further calcination at 900 °C for 1 h, the intensity of these peaks became stronger. These extra peaks are consistent with the (1 0 1), (1 1 2) and (1 0 3) reflections of a body-centered tetragonal $Mn_3O_4$ lattice (JCPDS 80-0382). This revealed that the heat-treatment at 800 °C led to the formation of a second $Mn_3O_4$ phase.

Thus, the subsequent electrochemical tests were conducted on the deposited films calcined in the temperature range between 400 and 800 °C for 1 h and shown in Section 3.2.

### 3.2. Effect of calcination temperature on Li-ion transport of the deposited films

Fig. 2 shows the cyclic voltammograms obtained from $LiMn_2O_4$ films calcined at temperatures between 400 and

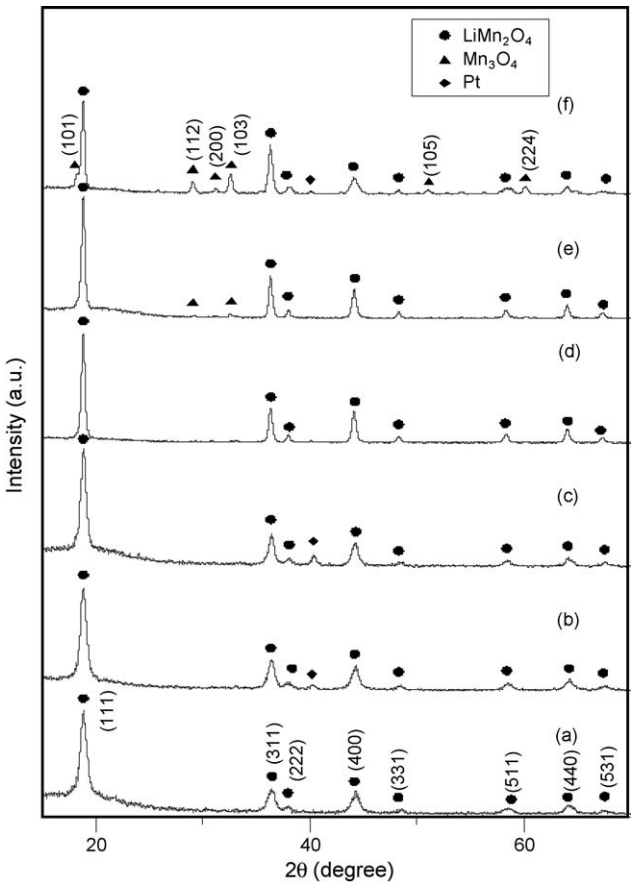


Fig. 1. GXRD traces of $LiMn_2O_4$ films calcined at different temperatures for 1 h: (a) 400 °C (b) 500 °C (c) 600 °C (d) 700 °C (e) 800 and (f) 900 °C.

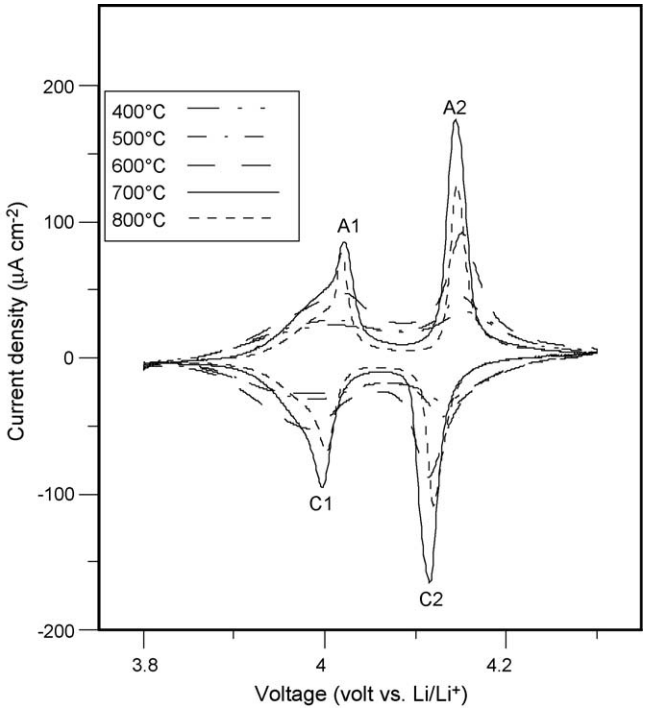


Fig. 2. Cyclic voltammograms obtained from the $LiMn_2O_4$ films calcined at different temperatures with a sweep rate of 0.2 mV $s^{-1}$.

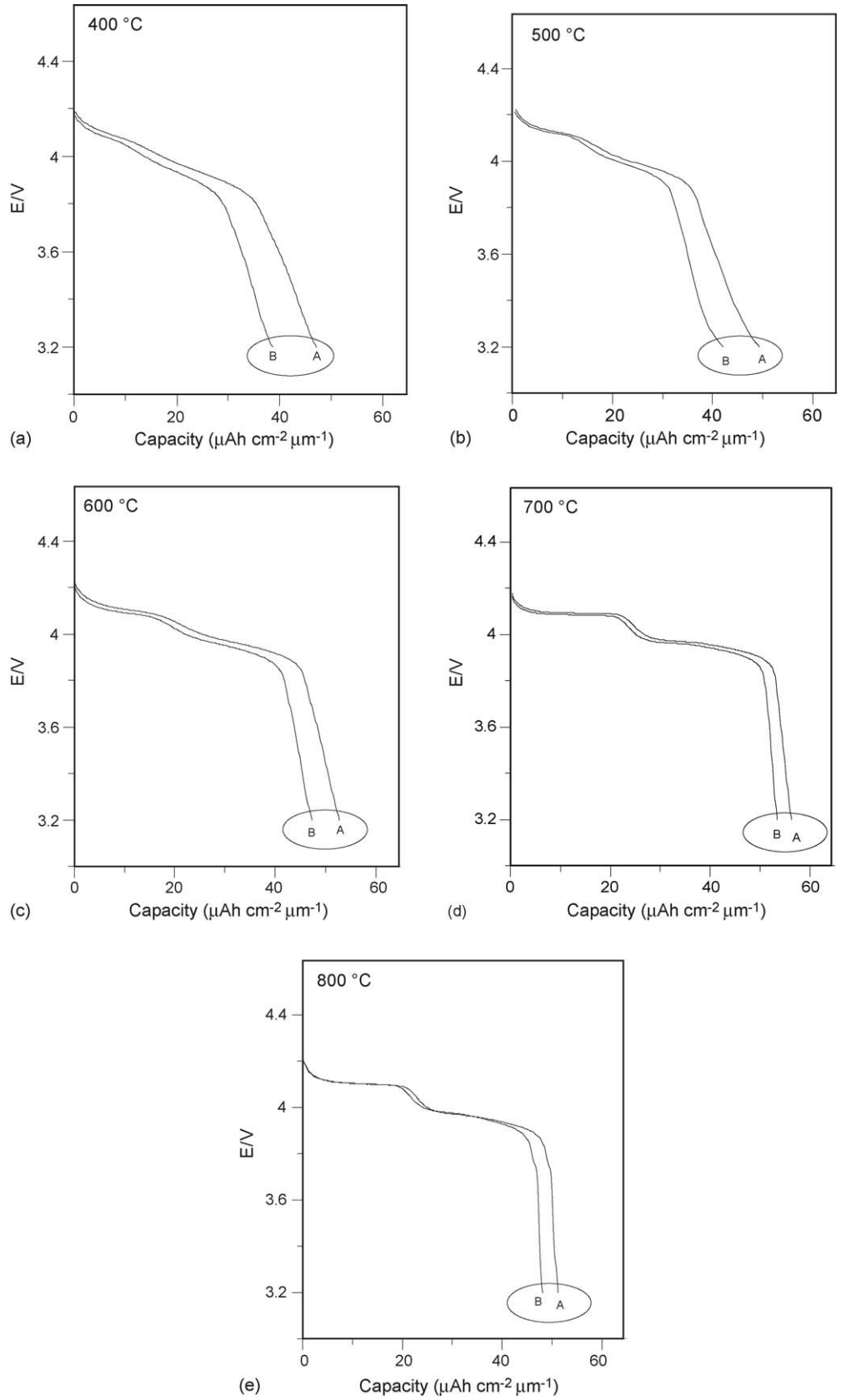


Fig. 3. Discharge curves of the $LiMn_2O_4$ thin-film cathodes calcined at different temperatures at a current density of (A) 20 μA $cm^{-2}$ and (B) 40 μA $cm^{-2}$.

Table 1
Kinetic properties for $LiMn_2O_4$ films calcined at different temperatures

| Calcination temperature (°C) | A1 | A2 | C1 | C2 (mV) |
|---|---|---|---|---|
| 400 | 42 | 24 | 41 | 22 |
| 500 | 29 | 17 | 29 | 17 |
| 600 | 22 | 16 | 22 | 15 |
| 700 | 12 | 10 | 11 | 13 |
| 800 | 8 | 8 | 9 | 8 |

800 °C for 1 h. All curves exhibited a couple of oxidation and reduction peaks located at about 4.00 and 4.13 V. This is a typical characteristic attributed to the (de)intercalation process of Li ion in 8a tetrahedral sites of $LiMn_2O_4$ spinel [11]. Moreover, these oxidation–reduction peaks became sharper when the calcination temperature was raised from 400 to 800 °C. This result indicated that the electrochemical response of the prepared $LiMn_2O_4$ films was highly dependent on the annealing temperature. A convenient diagnostic for these electrochemical reactions is the difference between the peak potential ($E_p$) and the potential at $I_{p/2}$ ($E_{p/2}$) [12]. The $E_p - E_{p/2}$ values for the calcined $LiMn_2O_4$ films, evaluated from the oxidation–reduction peaks in Fig. 2, are listed in Table 1. Obviously, the estimated $E_p - E_{p/2}$ values decreased with increasing calcination temperature for all oxidation–reduction peaks (A1, A2, C1 and C2). The narrower peak in the CV curve implies that a specific electrochemical reaction completes at a shorter period of time. In the present case, the narrower peak indicates that the (de)intercalation process of Li ion can take place at a more rapid rate. Fig. 3 shows the discharge curves as a function of current density of 20 and 40 μA $cm^{-2}$ for the $LiMn_2O_4$ films calcined at different temperatures. As is seen in Fig. 3, all discharge curves exhibited two discharge plateaus occurring at 4 V, which coincide with the results of CV plot (Fig. 2). In addition, it was also found that the $LiMn_2O_4$ film calcined at a high temperature has a better rate performance than one calcined at a low temperature. This may be attributed to the fact that the Li-ion diffusivity of $LiMn_2O_4$ film calcined at a high temperature is higher than that at a low temperature. Thus, both CV and PSCA measurements were carried out to evaluate the Li-ion diffusion coefficient of the $LiMn_2O_4$ thin-film cathodes calcined at various temperatures.

Fig. 4a shows the cyclic voltammograms of $LiMn_2O_4$ film calcined at 700 °C for 1 h recorded under different sweep rates. It was found that the anodic and cathodic peaks shifted to higher and lower potential and the peaks current ($I_p$) also increased when the potential sweep rate ($\upsilon$) increased from 0.05 to 0.8 mV $s^{-1}$. In the case of semi-infinite diffusion, the peak current is proportional to the square root of the sweep rate and the apparent diffusion coefficient of Li ion can be calculated from the relationship between a peak current and potential sweep rate [12]

$$I_p = (2.69 \times 10^5) n^{3/2} a D_{Li}^{1/2} C_{Li}^{*} \upsilon^{1/2} \quad (1)$$

where $I_p$ is the peak current (A), $n$ the number of electrons per reaction species (for Li ion, it is 1), $a$ the electrode area (1 $cm^2$), $D_{Li}$ the apparent diffusion coefficient of Li ion in a solid state electrode ($cm^2$ $s^{-1}$), $C_{Li}^{*}$ the bulk concentration of Li ion in the electrode (0.023 mol $cm^{-3}$ for $LiMn_2O_4$) and $\upsilon$ is the potential sweep rate (V $s^{-1}$). In the present case, as is shown in Fig. 4b, $I_p$ is linearly proportional to $\upsilon^{1/2}$. Thus, the diffusion coefficients corresponding to A2 and C2 peaks calculated from the slope of the linear fit are $4.46 \times 10^{-12}$ and $4.73 \times 10^{-12}$ $cm^2$ $s^{-1}$, respectively.

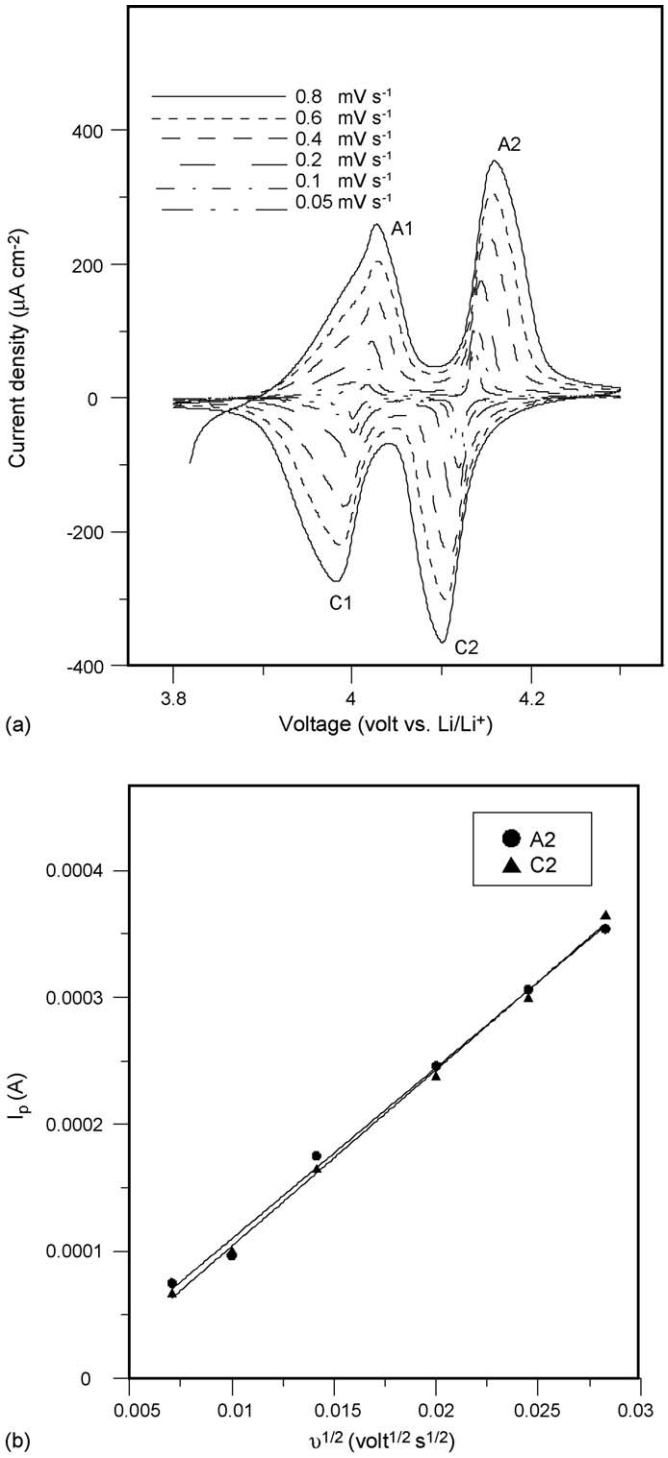


Fig. 4. (a) Cyclic voltammograms of $LiMn_2O_4$ film calcined at 700 °C for 1 h under various potential sweep rates, $\upsilon$. (b) Dependence of $I_p$ plotted as a function of $\upsilon^{1/2}$.

Table 2
Summary of the estimated diffusion coefficients of $LiMn_2O_4$ films calcined at different temperatures based on both cyclic voltammetry (CV) and potential step chronoamperometry (PSCA) methods

| Calcination temperature (°C) | CV | | PSCA ($\times 10^{-12}$ cm$^2$ s$^{-1}$) |
|---|---|---|---|
| | A2 | C2 | |
| 400 | 0.78 | 0.65 | 1.23 |
| 500 | 1.55 | 1.52 | 1.36 |
| 600 | 3.04 | 3.05 | 1.42 |
| 700 | 4.46 | 4.73 | 1.55 |
| 800 | 4.21 | 4.37 | 1.53 |

Although CV can provide the apparent $D_{Li}$ for $LiMn_2O_4$ thin-film cathode, a more accurate $D_{Li}$ in specific voltage can be obtained via the potential step chronoamperometry method. In a typical PSCA experiment, a potential step from 4.14 to 4.15 V (corresponding to the second anodic peak, A2, Fig. 2) was applied to the $LiMn_2O_4$ thin-film cathode calcined at 700 °C for 1 h and the measured current was recorded as a function of time. The dependence of resultant current ($I$) versus time ($t$) is shown in Fig. 5a. For a long time ($t \gg L^2 D_{Li}$), the following equation could be used to evaluate the Li ion diffusion coefficient [13,14]

$$\ln I(t) = \ln \frac{2\Delta Q D_{Li}}{L^2} - \frac{\pi^2 D_{Li} t}{4L^2} \quad (2)$$

where $\Delta Q$ is the amount of charge injected into the electrode, $D_{Li}$ the diffusion coefficient of Li ion and $L$ the thickness of film. According to Eq. (2), the $D_{Li}$ can be calculated from the linear slope of ln $I$ versus $t$ and the corresponding plot is shown in Fig. 5b. In the time domain, $t > 400$ s, the data were linearly fitted and the diffusion coefficient of Li ion for $LiMn_2O_4$ thin-film calcined at 700 °C for 1 h, evaluated from the slope ($\pi^2 D_{Li}/4L^2$), was $1.55 \times 10^{-12}$ cm$^2$ s$^{-1}$.

Similar CV and PSCA experiments were also conducted on other $LiMn_2O_4$ films calcined at 400, 500, 600 and 800 °C for 1 h and subsequent analyses were also carried out. The estimated $D_{Li}$, based on both CV and PSCA experiments are listed in Table 2. According to the published works [3–4,15–19], the Li-ion diffusion coefficient of the $LiMn_2O_4$ films was in the order of magnitude of −10 to −13. In this work, the estimated values were approaching to the published ones, indicating that the estimated Li-ion diffusion coefficients can be used as an appropriate indicator for Li ion transport in the calcined $LiMn_2O_4$ films obtained in this work. As is seen in Table 2, regardless of CV or PSCA experiments, the estimated $D_{Li}$ gradually increased to maximum when the calcination temperature was raised from 400 to 700 °C and subsequently decreased with increasing the temperature to 800 °C. Such a trend in the Li-ion diffusion coefficient can explain why the $LiMn_2O_4$ thin-film cathode calcined at 700 °C for 1 h exhibits the best rate performance.

### 3.3. Dependence of Li-ion diffusion coefficient versus crystallographic property of $LiMn_2O_4$ film

In Section 3.2, it was recognized that the Li-ion diffusion coefficient of the calcined $LiMn_2O_4$ films was dependent on the calcination temperature. The results of GXRD traces in Fig. 1 also showed that the calcination temperature indeed influenced the crystallography of $LiMn_2O_4$ films. Thus, it is inferred that the variation of the Li-ion diffusion coefficient for the $LiMn_2O_4$ films calcined at different temperatures may be related to the crystal characteristics of the $LiMn_2O_4$ films. Fig. 6a shows the

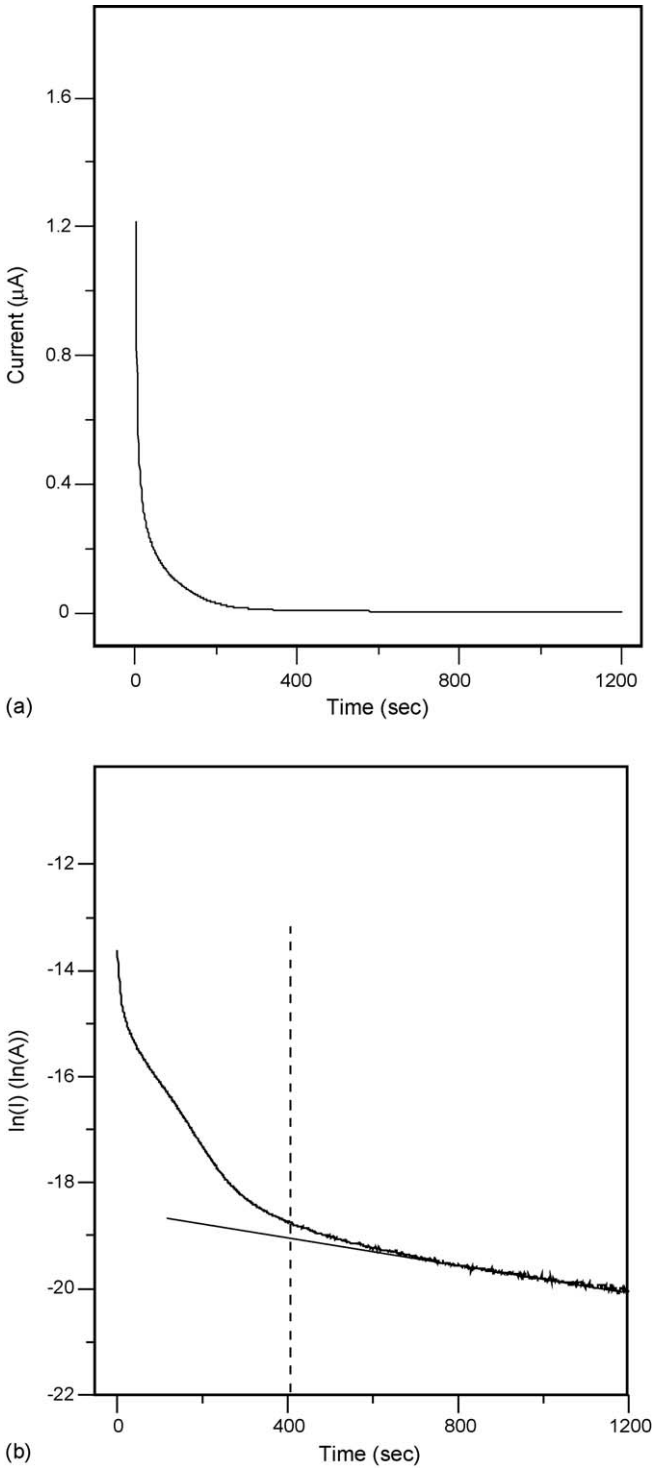


Fig. 5. (a) Current transient of $LiMn_2O_4$ thin-film cathode calcined at 700 °C for 1 h from the PSCA measurement in the potential range 4.14–4.15 V vs. Li/Li$^+$. (b) Plot of ln $I$ vs. $t$ from the PSCA measurement.

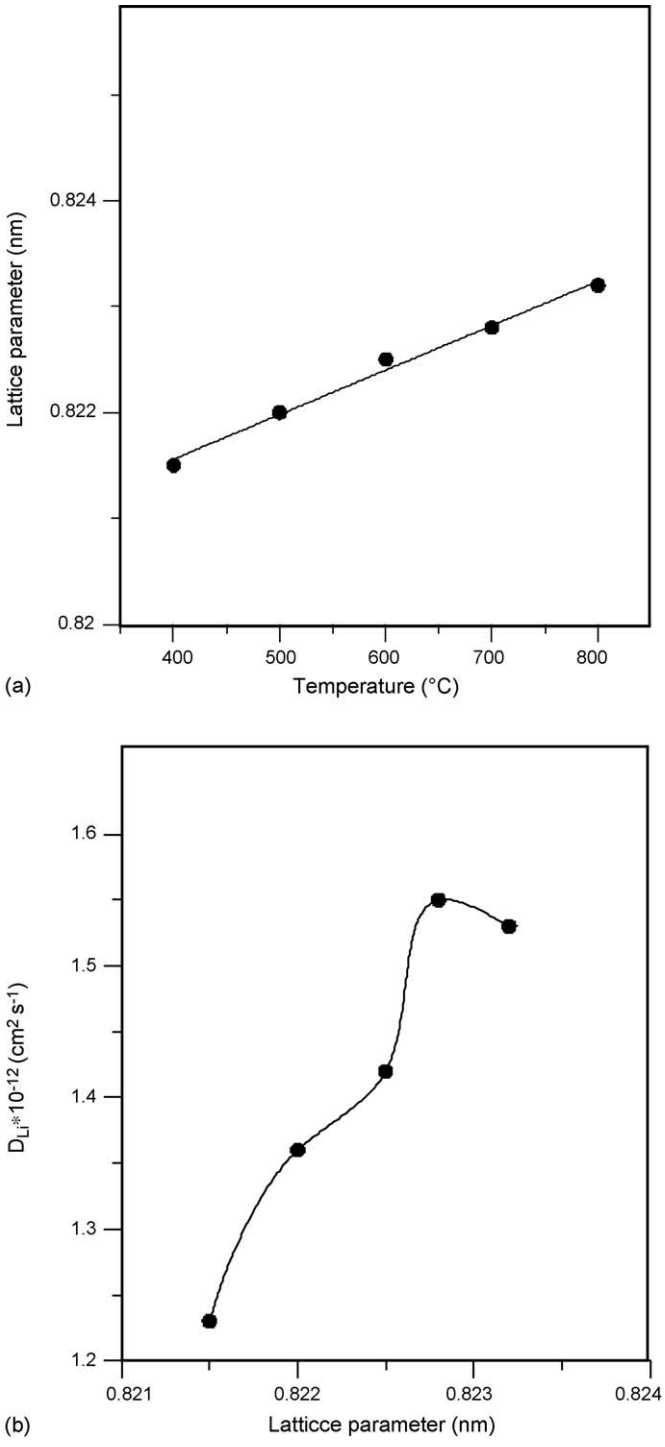


Fig. 6. (a) Effect of the calcination temperature on the lattice parameter of $LiMn_2O_4$ films. (b) Dependence of the Li-ion diffusion coefficient plotted as a function of lattice parameter of $LiMn_2O_4$ films.

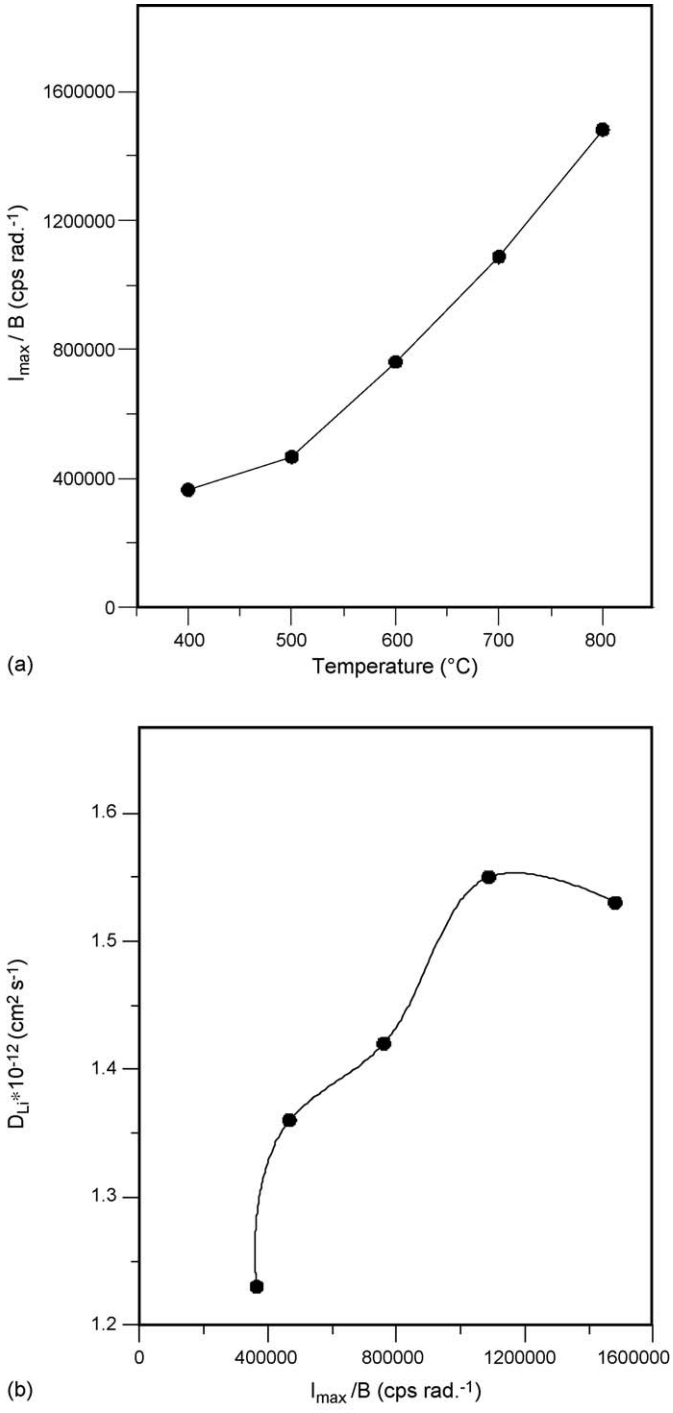


Fig. 7. (a) Effect of the calcination temperature on the crystallinity of $LiMn_2O_4$ films (b) Dependence of the Li-ion diffusion coefficient plotted as a function of the crystallinity of $LiMn_2O_4$ films.

variation of the lattice parameter of the $LiMn_2O_4$ films with the calcination temperature. The lattice parameter of the calcined $LiMn_2O_4$ films increased from 0.812 to 0.823 nm when the calcination temperature was raised from 400 to 800 °C.

Cubic $LiMn_2O_4$ spinel (space group $Fd3m$) is composed of three-dimensional framework of edge-sharing $MnO_6$ octahedral with lithium ions at tetrahedral sites, which share common faces with four neighboring empty octahedral sites at the 16c position. Such an atomic arrangement structure can provide the interstitial space for Li ion migration via a 16c–8a–16c transport paths during (de)intercalation process. Thus, it is suggested that Li ion transport is dependent on the size of interstitial space. The larger interstitial space would facilitate the migration of Li ions. Fig. 6b illustrates the variation of the Li-ion diffusion coefficient versus lattice parameter. Among the calcined $LiMn_2O_4$ films at the

temperatures of 400–700 °C, the $D_{Li}$ increased with the lattice parameter and the $LiMn_2O_4$ film calcined at 700 °C showed the highest Li-ion diffusion coefficient of $1.55 \times 10^{-12}$ cm$^2$ s$^{-1}$.

In addition to the interstitial space, the other factor that may affect the Li ion transport is the crystallinity of $LiMn_2O_4$ films. Tsumura et al. have pointed out that the displacement of Li ion from 8a sites to 16d sites and the formation of vacancies of manganese sites (16d) took place for the $LiMn_2O_4$ host with low crystallinity [20,21]. The crystal imperfection may block the Li ion migration. It is known that the crystallinity is proportional to the sharpness of the diffraction peak of XRD pattern. In a published work [22], Ahn and Song introduced a crystalline index ($I_{max}/B$) to numerate the XRD peak sharpness, where $I_{max}$ is the maximum intensity of a diffraction peak and $B$ is the width at the intensity equal to half $I_{max}$. In the present case of $LiMn_2O_4$ films calcined at different temperatures, the crystalline index was employed to estimate the crystallinity of the calcined films, and the results are shown in Fig. 7a. It showed that the crystallinity increased with increasing calcination temperature. Moreover, the variation of the Li-ion diffusion coefficient with the crystallinity of the calcined films is shown in Fig. 7b. It can be seen that the estimated $D_{Li}$ shows a positive relationship with the crystallinity of the calcined $LiMn_2O_4$ films when the calcination temperature was lower than 700 °C.

Although the 800 °C-calcined film has the largest lattice parameter and the highest crystallinity, the formation of electrochemically non-active $Mn_3O_4$ phase (Fig. 1e) may suppress the Li ion migration. Thus, the 700 °C-calcined $LiMn_2O_4$ film exhibits the highest Li-ion diffusion coefficient and best rate performance.

## 4. Conclusions

Based on the results of this work, the following conclusions may be drawn:

1. The Li-ion diffusion coefficient, $D_{Li}$, of the prepared $LiMn_2O_4$ films is strongly dependent on the calcination temperature. The measured value of $D_{Li}$ increases from $1.23 \times 10^{-12}$ cm$^2$ s$^{-1}$ for the film calcined at 400 °C for 1 h to $1.55 \times 10^{-12}$ cm$^2$ s$^{-1}$ for the one calcined at 700 °C for 1 h.
2. The $LiMn_2O_4$ film calcined at 700 °C for 1 h exhibits the best rate performance, which is due to the fact that the 700 °C-calcined one possesses the highest Li-ion diffusivity among all calcined films.
3. The highest Li-ion diffusion coefficient of the 700 °C-calcined $LiMn_2O_4$ film is attributed to the larger interstitial space and better crystal perfection in the $LiMn_2O_4$ lattice.

## Acknowledgement

Financial support by the National Science Council of the Republic of China under grant NSC 94-2120-M-006-002 is gratefully acknowledged.

## References

[1] H.S. Moon, J.W. Park, J. Power Sources 119–121 (2003) 717.
[2] K.F. Chiu, H.H. Hsiao, G.S. Chen, L.H. Liu, L.J. Her, H.C. Lin, J. Electrochem. Soc. 151 (2004) 452.
[3] C. Julien, E. Haro-Poniatowski, M.M. Camacho-Lopez, L. Escobar-Alarcon, J. Jimenez-Jarquin, Mater. Sci. Eng. B72 (2000) 36.
[4] K.A. Striebel, A. Rougier, C.R. Horne, R.P. Reade, E.J. Cairns, J. Electrochem. Soc. 146 (1999) 4339.
[5] C.H. Chen, E.M. Kelder, J. Schoonman, J. Power Sources 68 (1997) 377.
[6] M. Mohamedi, D. Takahashi, T. Uchiyama, T. Itoh, M. Nishizawa, I. Uchida, J. Power Sources 93 (2001) 93.
[7] Y.J. Park, J.G. Kim, M.K. Kim, H.T. Chung, H.G. Kim, Solid State Ionics 130 (2000) 203.
[8] Y.H. Rho, K. Kanamura, T. Umegaki, J. Electrochem. Soc. 150 (2003) A107.
[9] X.M. Wu, X.H. Li, Z. Wang, Z.B. Xiao, J. Liu, W.B. Yan, Mater. Chem. Phys. 83 (2004) 78.
[10] F.Y. Shih, K.Z. Fung, J.W. Wang, J. Alloy. Compd. 407 (2006) 282.
[11] Y. Gao, J.N. Reimers, J.R. Dahn, Phys. Rev. B45 (1996) 3878.
[12] A.J. Bard, L.R. Faulkner, Electrochemical Methods, John Wiley & Sons, New York, 1980.
[13] C.J. Wen, B.A. Boukamp, R.A. Huggins, W. Weppner, J. Electrochem. Soc. 126 (1979) 2258.
[14] M.D. Levi, D. Aurbach, J. Phys. Chem. B101 (1997) 4641.
[15] C. Liquan, J. Schoonman, Solid State Ionics 67 (1994) 17.
[16] K.A. Striebel, C.Z. Deng, S.J. Wen, E.J. Cairns, J. Electrochem. Soc. 143 (1996) 1821.
[17] A. Rougier, K.A. Striebel, S.J. Wen, E.J. Cairns, J. Electrochem. Soc. 145 (1998) 89.
[18] D. Shu, K.Y. Chung, W.I. Cho, K.B. Kim, J. Power Sources 114 (2003) 253.
[19] S.D. Das, S.B. Majumder, R.S. Katiyar, J. Power Sources 139 (2005) 261.
[20] T. Tsumura, A. Shimizu, M. Inagaki, Solid State Ionics 90 (1996) 197.
[21] T. Tsumura, M. Inagaki, Solid State Ionics 104 (1997) 35.
[22] D. Ahn, M.Y. Song, J. Electrochem. Soc. 147 (2000) 874.